Weather Responsive Ventilation for Residential Energy Efficiency and Indoor Air Quality

Final Report

Submitted to:
Kentucky Rural Energy Consortium

January 11, 2008

By:

Donald Colliver, Ph.D., P.E.
University of Kentucky
128 C.E. Barnhart Building
Lexington, KY 40546-0276
859.257.3000 x211
colliver@bae.uky.edu

and

James Bush, Ph.D. Student
University of Kentucky
128 C.E. Barnhart Building
Lexington, KY 40546-0276
859.257.3000 x205
james.bush@bae.uky.edu

Original Proposal Objectives

The goal of the research is to develop a weather responsive ventilation (WRV) control system to optimize the fan flow rate bringing in outdoor air as the conditions warrant – increasing the flow when weather data suggests a small or even negative energy liability and decreasing the flow as the liability rises. Knowledge of past performance and anticipated behavior will ensure that minimum fresh air requirements are continually achieved. The research goal fits solidly in the research plans of the Department of Energy and the Energy Policy Act of 2005 which seek to make progress toward net zero-energy buildings by developing cost effective technologies that reduce energy consumption and create healthy indoor environments.

The objectives necessary to achieve this goal are divided among four project areas: simulations, system calibration, test cell experiments, and field testing. Computer simulations will identify regional potential for energy savings by investigating how building parameters and local climate impact ventilation performance. Influential parameters found will be combined with different weather-sensitive optimization strategies to evaluate ventilation control algorithms for testing. The optimal algorithm found will be programmed into a microcontroller that will regulate the flow of a fan; and the response of the system to simulated weather conditions will be calibrated in a laboratory environment. The performance of the prototype system will then be evaluated on external test cells using a statistically designed experiment. Natural ventilation, weather responsive ventilation, and fixed-flow ventilation treatments will be compared. Lastly, the prototype system will be installed in a full-scale, highly instrumented residential test home at a national laboratory. The building air exchange and associated energy load will be monitored as the system alternates between fixed-flow and weather responsive ventilation modes.

Variance from Plan

Early in the research, the investigators determined that existing models for estimating natural air exchange or *infiltration*, i.e. air movement into a building induced by pressures from wind and temperature, were inadequate for the desired objectives. Because the purpose of a WRV system is to supplement natural air exchange, failure to accurately predict this quantity severely undermines the efficacy of the system. As a result, the investigators made a conscious decision to move the focus of the research toward improved modeling of infiltration and infiltration with the addition of mechanical ventilation. The consequence of this focus shift required a revision to the test methodology to permit near real-time monitoring of air flow movement via pressure differential measurement. By comparison, ventilation performance is typically evaluated using longer term tracer gas measurement techniques.

Of the four research areas identified above, the project was able to largely complete the first three (simulations, calibration and experiments), however, additional analysis of the data is necessary before field testing can be initiated. Results and achievements stemming from the research are presented in the following sections.

Research Area I – Calibration

To measure air flow, it was decided to rely on a pressure differential measurement across a flat, square-edged orifice plate. The technique was preferred because it offered a low cost option with bi-directional capability – a critical feature when measuring natural flows that both enter and exit building openings depending on the direction of the driving force.

Published data on flat orifice behavior is not reliable for the low pressure, low air flow rates typical of residential ventilation design. It was thus necessary to develop calibrated orifice flow behavior for the size and pressure differential expected in the experimental phase of the research. To accomplish this, the air flow calibration chamber at the University of Kentucky, Department of Biosystems & Agricultural Engineering was repaired and updated with differential pressure transducers coupled to a Measurement Computing USB-1408FS analog and digital I/O module and controlled by the Visual Basic data acquisition and processing program shown in Figure 1. The numerical processing and the air flow calibration chamber adhere to ANSI/ASHRAE Standard 51-1999 Laboratory Methods of Testing Fans for Aerodynamic Performance Rating.

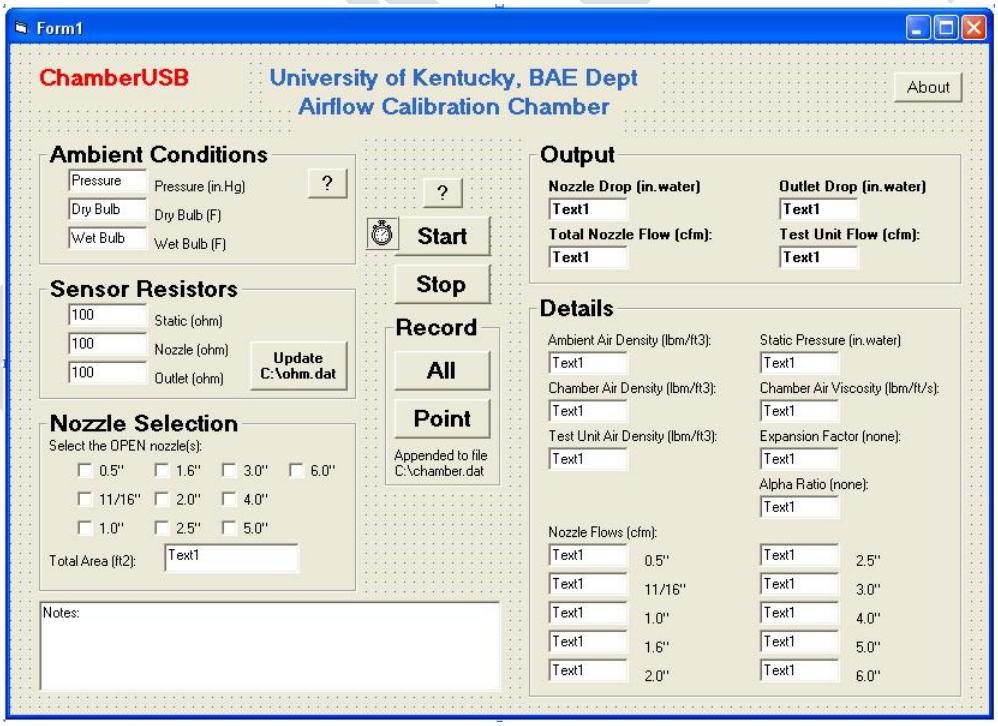

Figure 1: Air Flow Calibration Data Acquisition System Interface

Two sizes of orifice plates were calibrated: 3.0 inch plates to be mounted in walls of the test units and 2.0 inch plates to monitor air flow supplied by mechanical ventilation systems. The 3" plates were tested under very low conditions (less than 0.25 in.wc), consistent with the pressures induced by head-on winds less than 30 miles an hour and were sized to approximate

the flow that might be experienced by a modest sized residential home. The 2" plates, intended to monitor fan flows up to 50 cfm, were tested up to 0.8 in.wc.

To facilitate measurement and analysis, replicates were statistically tested to insure that plates were interchangeable and that they exhibited consistent, bi-directional behavior. The results of the calibration tests, standardized to dry air at 59°F at sea level, were fit to the flow equation

$$Q = C\,\Delta P^{n} \tag{1}$$

where Q is the flow in cubic feet per minute (cfm) and ΔP is the pressure drop in inches of water. C and n represent physical properties of the opening. C relates the area and discharge coefficient of the opening while n indicates the flow behavior from turbulent (n = 0.5) to laminar (n = 1.0). The statistical results are shown in Table 1 along with the values that would be expected from an idealized sharp-edged orifice plate. Pressure-Flow response curves for the orifice plates are shown in Appendix A.

Table 1: Calibration Parameters for Sharp-Edged Orifice Plates

Orifice Diameter (inches)	C (cfm/in.wc^n)	n (--)	95% confidence (± cfm)
2.0	59.1	0.49	0.5
Idealized	52.0	0.50	--
3.0	119.4	0.48	0.7
Idealized	116.9	0.50	--

The results compare favorably with the idealized theory. The high confidence, less than 1 cfm, speaks to the value of the data acquisition system and the repeatability of the air flow chamber. Nonetheless, confidence of the flow measurement under test conditions will decrease according to the accuracy of the pressure sensor in use.

Research Area II – Superposition Experiments

The net amount of outside air introduced into a home from the combined sources of infiltration and mechanical ventilation is not easily determined. The two sources are each capable of altering the pressure differential across the envelope and thus do not act independently. Moreover, the relationship is altered by the type of mechanical ventilation system being used, be it an exhaust, supply, or balanced system. The additive manner in which infiltration and mechanical ventilation are combined is known as *superposition*.

Given the uncertainty surrounding natural-mechanical superposition and recognizing that superposition is the essence of a WRV system, a process for combining infiltration and mechanical ventilation needed to be developed. This phase of this research project was designed to monitor the air exchange rates experienced by test units with and without mechanical ventilation in order to develop a reliable superposition model.

The test units consisted of three 8' cubes mounted on the roof of the Biosystems & Agricultural Engineering building. The calibrated 3" orifice plates were installed at mid-height on each side of the test units allowing for the simultaneous measurement of air flow in or out of each face. Although unlikely in an unconditioned building, positioning the orifice plates at the neutral axis removed the potential for flow from stack effects (i.e. temperature). Thus air flow could be attributable to wind-induced pressures only. Uncontrolled leakage from cracks in the test units is considered negligible. Multiple leakage tests indicated that uncontrolled leakage area was about 5% of the area presented by the four orifice plates and is distributed throughout the envelope. Mechanical ventilation was supplied by a Fantech FR100 centrifugal fan blowing air through a calibrated 2" orifice plate. An image of the test units is presented in Figure 2. A mechanical fan is shown at the bottom of the center test unit.

Figure 2: Experimental Test Units (looking South)

Wind pressure, the independent variable driving air flow across the orifice plates, was measured using a Vaisala WXT510 Weather Station. The weather station uses ultrasonic triangulation to determine wind speed and direction while an internal sensor provides temperature, humidity and ambient pressure. The weather station was located on the southwest corner of the roof deck at the height of the orifice openings.

Data acquisition and processing was performed using a Visual Basic program to interface with a Measurement Computing PCI-DAS6036 analog and digital module and the WXT510 via RS232 communication protocol. The PCI board provided simultaneous sampling of up to 14 pressure transducers (4 on each unit plus 2 ventilation fans) while the WXT510 provided wind speed, wind direction and ambient air density. Synchronization between the PCI and the WXT510 was possible to within 1 second, but no less due to internal updating of the WXT510 measurement parameters. The testing protocol is given in Figure 3.

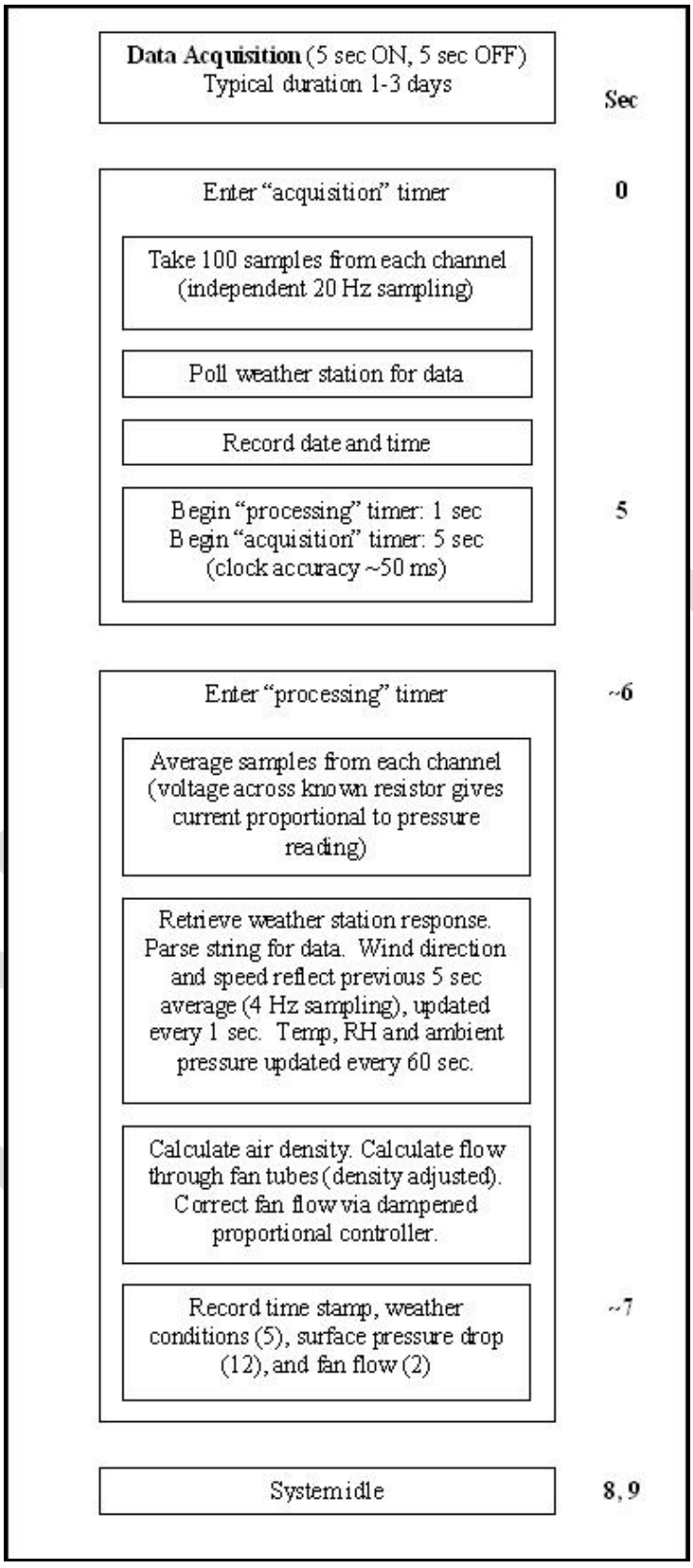

Figure 3: Measurement Protocol for Superposition Experiments

Testing was conducted in two stages. The first stage was a "training" period in which the test units were calibrated to determine their natural response in the absence of any mechanical ventilation. In the second stage, one of three levels of mechanical ventilation (15- 30- or 45 cfm) and the response measured. Analysis of the natural and mechanical treatments would be used to formulate a reliable superposition model.

Experiments were run over much of 2007. The training period lasted the longest and was used to gain familiarity with the setup and establish a basis for the test protocol. Over 430,000 usable data sets were collected for processing. Two unavoidable issues, cited in Figure 4, were encountered which merited special attention: (1) water intrusion to the pressure lines from rain and (2) long-term drift of a sensor's zero position.

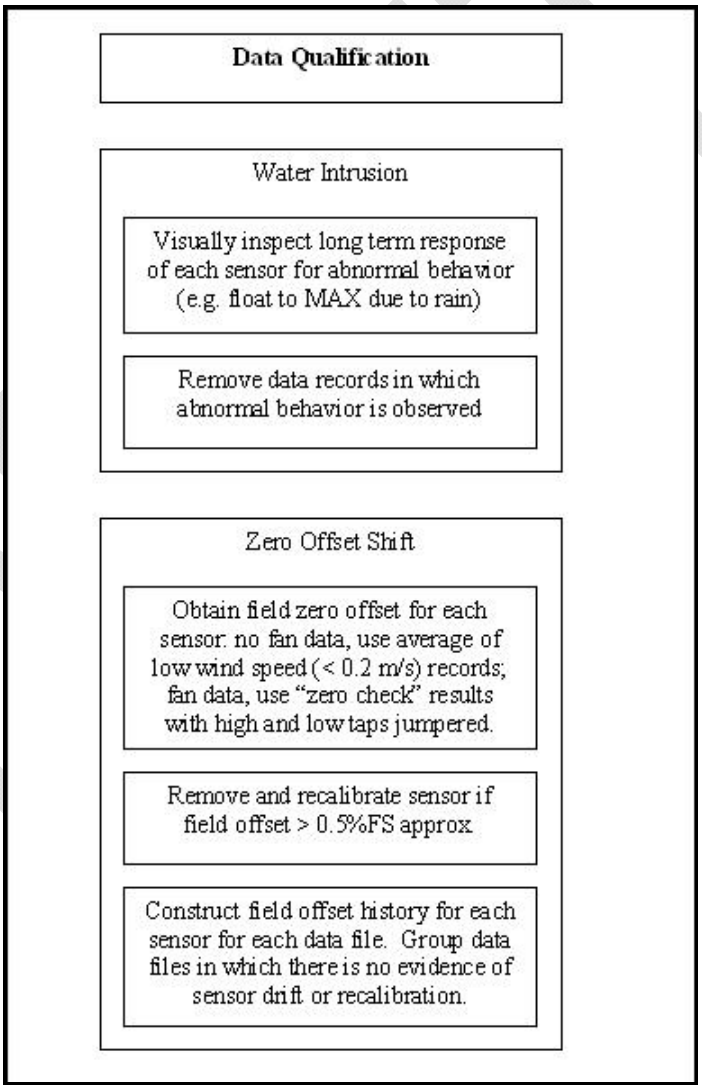

Figure 4: Data Qualification Procedure

During the second stage of testing, mechanical ventilation was added. For each fan speed, approximately 50,000 data records were collected per unit. Interspaced with the fan tests was at least one "no fan" condition to be used as a repeatability check against the original training data.

Early review of the data concluded that treating each record set individually would be problematic. The inherent variability in wind movement, especially around structures, combined with extremely low pressure readings on at least one face of a test unit, created total air exchange error readings on the order of 20% or more. To resolve the issue, an averaging technique was employed to condense record sets sharing the same wind speed and wind direction within 5 degrees of one another. The technique, outlined in Figure 5, successfully captured the response of the test units while making the large data set considerably more manageable.

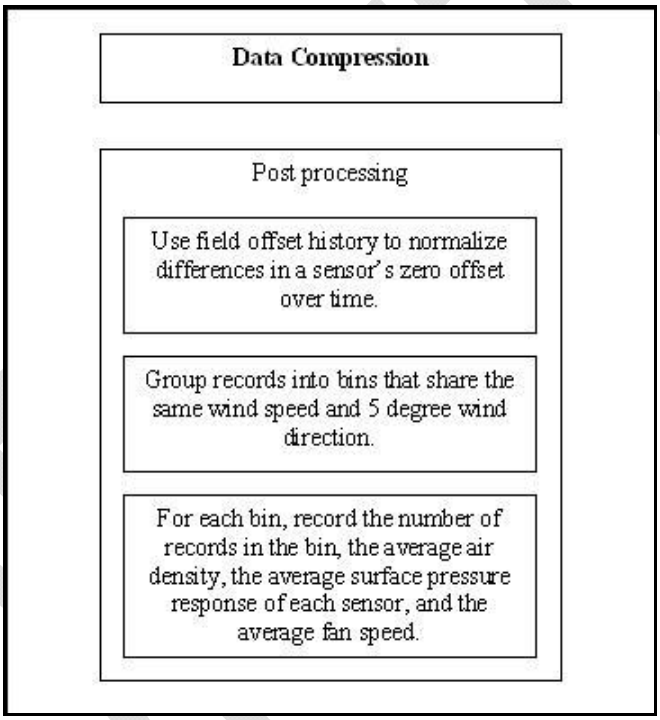

Figure 5: Data Averaging Method

The data was analyzed using SAS statistical software. Conventional air flow behavior would expect a linear relationship between the pressure acting on the surface of a test cell at a given angle (P_s) and the free stream wind velocity pressure ($\frac{\rho U^2}{2}$):

$$P_s(\theta) = Offset + C_p(\theta)\frac{\rho U^2}{2} \quad (2)$$

In this equation, θ is the wind approach angle measured in degrees relative to the surface normal, ρ is the air density and U is the wind speed. The *Offset* is a fan induced pressure shift, independent of wind direction. $C_{p,\theta}$ is the wind-induced indoor-outdoor surface pressure coefficient which will change with the wind's approach angle. A head-on wind (θ = 0°) would

be expected to create the maximum positive pressure. Conversely, a negative pressure, $C_p < 0$, would be expected on either side ($\theta = 90°$) as the air stream accelerates around the structure.

The results of the statistical analysis confirmed the theory remarkably well. A portion of the results for the Blue unit are provided in this report, but the general behavior was similarly confirmed by the other two units. Table 2 shows the *Offset* values determined for each surface of the Blue unit by treatment. The expected response that the *Offset* will increase at high fan speeds is clearly evident in the results. The values are generally negative because a supply fan was used which creates flow out of the test unit. The idealized value, provided for comparison, is the pressure drop that would be produced across the 3" orifice plate at one-quarter of the flow provided by the fan setting.

A plot of the indoor-outdoor pressure coefficient for the Blue-North surface is shown in Figure 6. The general curvature of the data is in good agreement with similar studies investigating building surface pressures. More importantly, the general agreement of the data demonstrates that Cp values act independently from mechanical fan pressures. Standard error averaged 0.05 for the data, peaking at 0.14 for the Medium treatment due to limited data points and variability near the $\theta = 100°$ condition.

Table 2: *Offset* Values by Treatment, Blue Unit

Surface	Treatment	Offset	Std Error	t-value
E	High	-1.57	0.03	-58.63
N	High	-1.43	0.03	-53.17
S	High	-1.67	0.03	-62.14
W	High	-1.87	0.03	-69.86
Idealized	High	-1.74	--	--
E	Low	-0.35	0.02	-14.29
N	Low	-0.03	0.02	-1.25
S	Low	-0.29	0.02	-11.81
W	Low	-0.69	0.02	-27.99
Idealized	Low	-0.17	--	--
E	Medium	-1.08	0.03	-38.92
N	Medium	-0.77	0.03	-27.71
S	Medium	-0.75	0.03	-27.07
W	Medium	-0.89	0.03	-32.11
Idealized	Medium	-0.74	--	--
E	Natural	-0.07	0.02	-3.3
N	Natural	0.26	0.02	12.26
S	Natural	0.00	0.02	0.18
W	Natural	-0.20	0.02	-9.66
Idealized	Natural	0.00	--	--
E	Natural	0.05	0.03	1.83
N	Natural	0.28	0.03	10.44
S	Natural	-0.11	0.03	-4.08
W	Natural	-0.26	0.03	-9.64
Idealized	Natural	0.00	--	--

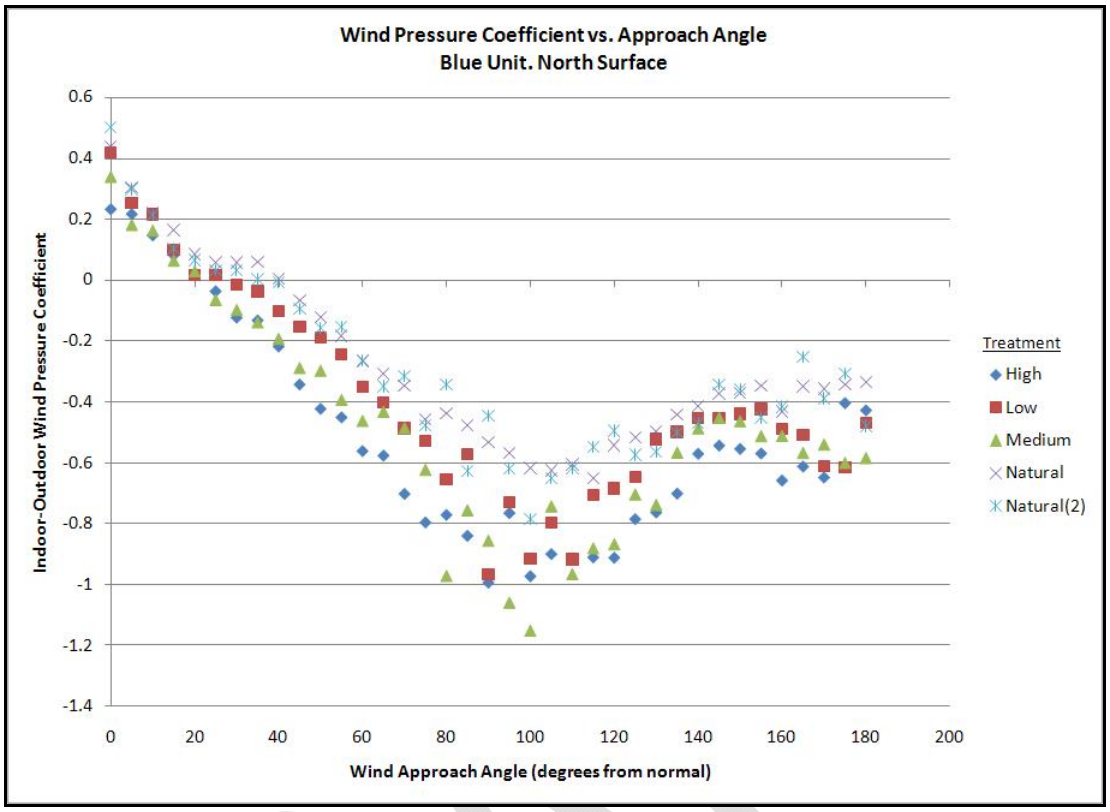

Figure 6: Blue-North Wind Induced Surface Pressure Coefficient

The preceding analysis provided a novel way to estimate total air infiltration into buildings. Whereas previous work concentrated on relating flow to wind speed directly, the approach used in this research applies fundamental pressure relationships from which flow rates can be derived. By applying the results of the analysis to Equations 1 and 2, the total air flow in (or out) of a test unit can be estimated from three parameters: wind speed, wind direction and fan flow.

To test the concept, the approach was applied to the natural data sets using a wind speed of 4 m/s. The results, presented in Figure 7, show the percent difference in the total air flow entering the unit and the total air flow exiting the unit. A certain level of discontinuity is expected when calculating four air flows independently, yet the results (within ±20%) are noteworthy considering the error typically associated with low pressure/low flow measurements.

In addition, Figure 7 provides evidence of wind shadowing effects between the units. The curve for the Red unit is relatively flat from due south (180°) to due west (270°) because its shadowing is symmetrical (Blue on one side; Yellow on the other). The curve drops off at due south as the Red unit falls in the shadow of the Blue unit. The same behavior occurs at due west when the Red unit falls under Yellow's shadow. Similar behavior can be explained in the other curves based on the location of structures on the roof deck.

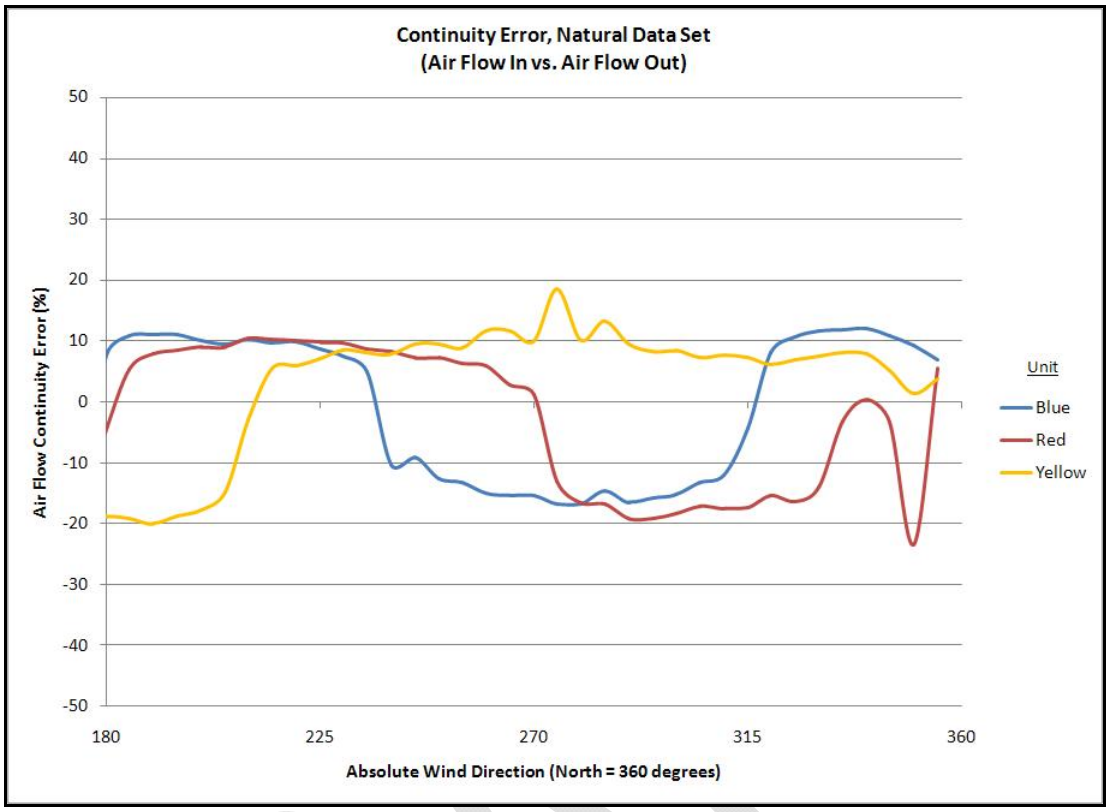

Figure 7: Flow Continuity Error, Natural Data Set

To improve the superposition technique and to reconcile the flow discontinuity, a convergence operation was added to the model. Recognizing that the internal pressure of a test unit is common to all surfaces, there is justification to shift the resultant of Equation 2 uniformly such that that flow continuity is achieved. As shown in Figure 8, the addition of the convergence operation greatly improved the model's ability to predict air infiltration resulting from combined natural and mechanical sources. Precise estimates would lie on the yellow line (slope = 1.0). By comparison, the UK – Continuity model has a slope of 0.98 whereas the conventional LBL model has a slope of 0.28.

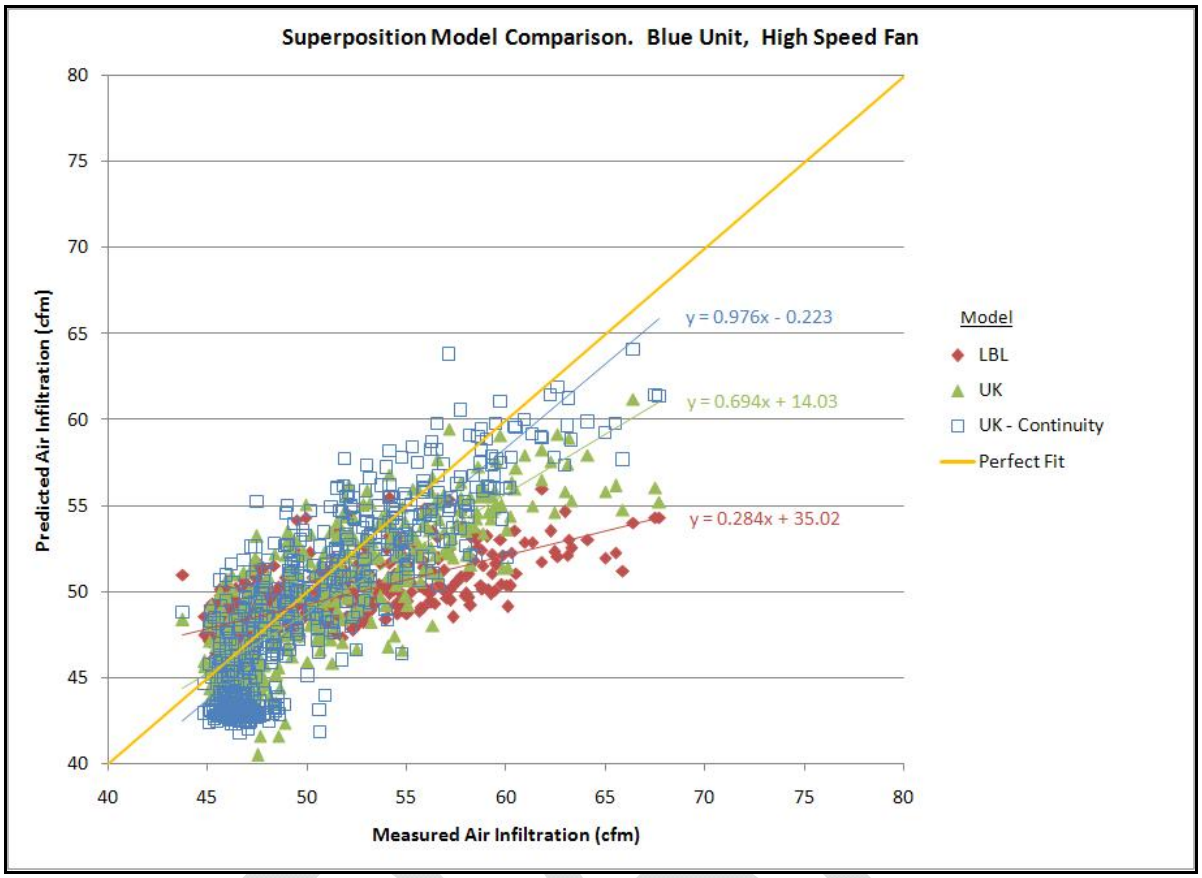

Figure 8: Superposition Model Comparison

Research Area III – Weather Factor Simulations

This area of research expands on the work begun by Yuill[1] by conducting a formal parametric analysis of the weather factor over a range of climates, leakage areas and building types. The weather factor is used to calculate the annual effective air exchange for a house with known leakage. It is a climate-specific index based on the air exchange induced by natural forces. As a metric for assessing indoor air quality, the weather factor makes a notable distinction between the average air exchange of a building and the *effective* air exchange. For the purposes of controlling long-term emissions, it is the average pollutant concentration over a period of time that is of interest. However, a linear relationship between the average pollutant concentration and the average ventilation rate only exists when the air exchange is constant. For variable ventilation, as exhibited by natural forces, the harmonic average of prior ventilation rates provides a superior assessment of indoor air quality. This rationale is embodied in Yuill's weather factor such that the effective air exchange it describes is a hypothetical steady-state condition that would result in the same average pollutant concentration over the same time period.

The procedure for calculating the weather factor is contained in Yuill's discussion of the development of ASHRAE Standard 136. For convenience, the methodology for calculating the weather factor is summarized below along with the governing equations:

1. Solve LBL model for hourly infiltration rate Q_{nat}

$$Q_{nat} = \frac{A_L}{1000}\sqrt{C_s \Delta T + C_w U^2}$$

natural infiltration rate

A_L effective leakage area (at 4 Pa)
C_s stack coefficient related to building height
C_w wind coefficient related to terrain and shielding
ΔT inside-outside temperature difference
U wind speed at eave height

2. Solve mass balance equation for hourly pollutant concentration C, assuming a constant source pollutant. The solution requires the initial concentration C_0 which is dependent on past air change rates. Hours in which the inside-outside temperature difference is less than 3°C are excluded from the calculation.

$$C = \frac{S}{Q}\left(1 - e^{\frac{-Qt}{V}}\right) + C_0 e^{\frac{-Qt}{V}}$$

pollutant concentration

S source strength (emission rate)
Q ventilation rate
C_0 initial pollutant concentration
V zone volume

3. Calculate average pollutant concentration $\overline{C}$ over the period of interest

[1] Yuill, G.K. 1991. The Development of a Method of Determining Air Change Rates in Detached Dwellings for Assessing indoor Air Quality. *ASHRAE Transactions*. 97(2): 896-903.

4. Calculate the effective ventilation as $Q_{eff} = S / \overline{C}$

   Note: Q_{eff} is not the average of $\overline{Q}_{nat}$ over the same time period (Sherman and Wilson 1986)

5. Calculate the effective air change rate $I = Q_{eff} / V$

6. Define weather factor W = I / A_n where A_n is the normalized envelope leakage

$$A_n = 0.1\left(\frac{A_L}{A_f}\right)\left(\frac{H}{H_0}\right)^{0.3}$$

normalized leakage area

A_L effective leakage area (at 4 Pa)
A_f floor area of building
H eave height of building
H_0 height of one story (2.5m)

7. Limited published data by Yuill shows W is essentially constant over range of A_n. A 10% difference was observed for $0.05 \le A_n \le 1.0$ with W increasing for lower A_n. Consequently, the weather factor presented in ASHRAE Standard 136 represents the conservative selection of $A_n = 1$ such that W = I for geographic locations.

A Visual Basic program was written to calculate the weather factor according to the methodology outline above. The primary differences between ASHRAE Standard 136 and this study are identified in Table 3.

Table 3: Weather Factor Study Comparison

Parameter	UK Study	ASHRAE Std 136
Weather file	SAMSON 30 year data	TMY data
Wind shelter	Classes iii, iv, v	Class iv
Normalized Leakage Area	$0.05 \le A_n \le 2.2$ 27 values representing 3 floor areas, 3 leakage areas and 3 building heights	$A_n = 1.0$ 1 value representing 1 building type
Time period	1-, 3-, 8- and 12-hour, Day, Week, Month, and Annual	Annual

The first step of the process was to perform quality and verification checks on the weather data itself. The eight cities selected for simulation runs, one from each of the DOE climate zones, is presented in Table 4. With one exception, the 30 years of SAMSON weather data was surprisingly robust. Phoenix was missing 25 hours of wind speed data which were filled using data from the previous day. During years when every third hour was recorded (a common practice in the 1960's), all three hours were assigned the first value.

Table 4: Selected Cities for Weather Factor Simulations

Climate Zone	City	WBAN
1	Miami, Fl	12839
2	Phoenix, AZ	23183
3	Memphis, TN	13893
4	Lexington, KY	93820
5	Chicago, IL	94846
6	Burlington, VT	14742
7	Duluth, MN	14913
8	Fairbanks, AK	26411

The 30-year weather data was used to calculate hourly natural air exchange rates and the associated pollutant concentration for the various building types. A second process was then conducted to translate the pollutant concentration values into weather factors for different time periods of interest. The entire process was computationally extensive. All told, over 117 million individual weather factor values were calculated.

At a macro level, the results of the UK study closely resemble those presented in ASHRAE Standard 136. The weather factor shown in Table 5 for the UK study represents the average value over all weather years, building types and wind shelter classes. The values in Standard 136 are typically within 10%, and with the exception of Zone 8, always higher. As a consequence, Standard 136 would overestimate the air change rate of a generic building.

Table 5: Annual Weather Factor Comparison for Selected Cities

Climate Zone	City	Weather Factor		Difference
		UK	Std 136	
1	Miami, Fl	0.65	0.69	6.2%
2	Phoenix, AZ	0.66	0.68	3.0%
3	Memphis, TN	0.71	0.78	9.9%
4	Lexington, KY	0.73	0.80	9.6%
5	Chicago, IL	0.84	0.93	10.7%
6	Burlington, VT	0.84	na	na
7	Duluth, MN	0.96	1.00	4.2%
8	Fairbanks, AK	0.91	0.90	-1.1%

The results also confirm that the weather factor is relatively constant over a range of normalized leakage areas, especially for values of $A_n > 0.5$. The trend, shown in Figure 9, is for a slight increase in the weather factor as the envelope tightens. The effect is more pronounced with greater exposure (e.g. wind shelter class iii).

Figure 9 highlights an important component of the UK study: there is a distinct and quantifiable difference in the weather factor based on wind shelter class. As the Lexington example demonstrates, the weather factor can vary by up to 25% with the change of a single wind shelter class. Similar behavior was found across all cities and weather years.

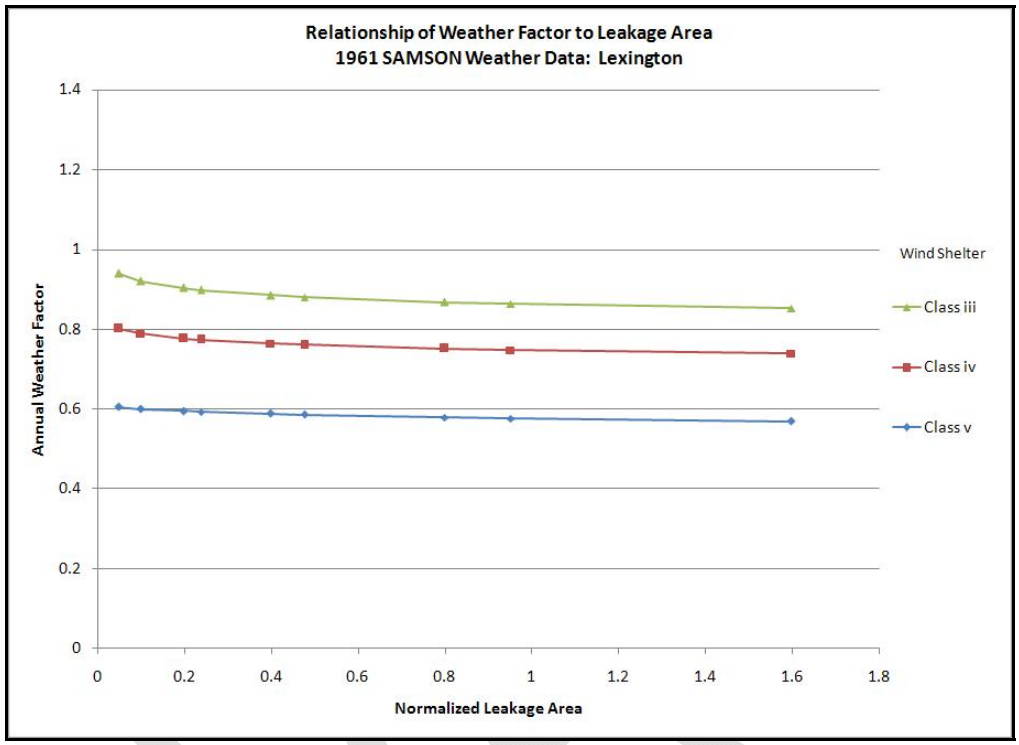

Figure 9: Relationship of Weather Factor to Leakage Area. Lexington, 1961.

The 30-year analysis further demonstrated that the year-to-year variation in the weather factor could be significant, on the order of 20 to 30% within a given wind shelter class. Using Lexington as an example again, Figure 10 shows the long-term variability of the weather factor by wind shelter class. The group variability on the right-hand side of the chart shows how much the weather factor might fluctuate if specific weather data and wind shelter information is not known. Results for the other cities are provided in Appendix B.

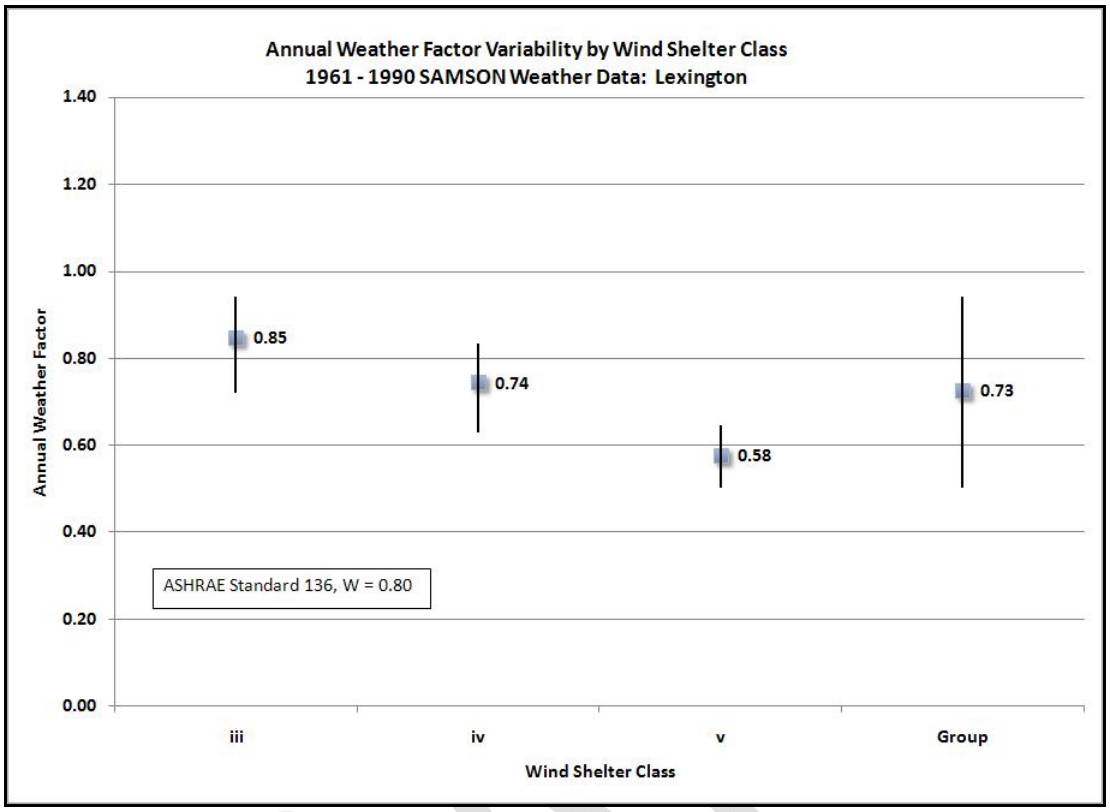

Figure 10: 30-Year Annual Weather Factor Variability, Lexington.

Shorter time periods exhibit even greater variability, so average values become even less meaningful. From this perspective, it is more appropriate to analyze the data from a percentile approach in order to provide some level of confidence to a particular weather factor. For example, Table 6 compares the 5th percentile hourly weather factors for Lexington to the annual weather factor for the same wind shelter class. From a design standpoint, where one might want to insure a reliable, minimum level of air exchange, Lexington's annual weather factor would need to be reduced by approximately 40%. Analysis on a seasonal basis and on the other cities is ongoing.

Table 6: Short- Versus Long-Term Weather Factor Comparison, Lexington.

Wind Shelter Class	P5 Weather Factor		Difference
	Annual	Hourly	
iii	0.85	0.51	-39.8%
iv	0.74	0.44	-40.3%
v	0.58	0.34	-42.2%

Looking Forward

The investigators would like to thank the Kentucky Rural Energy Consortium for their support and patience during the preceding 18 months. Despite the slow start, the project is contributing to the knowledge base of air flow modeling, climate-based design and hybrid ventilation strategies. The investigators anticipate completing the project over the next several months.

Two research goals that have not been completed are estimating the energy savings potential of a WRV and the validation of WRV performance. For the first task, the results of the superposition study will be integrated with a building energy simulation program in order to estimate the potential savings of a WRV system across different climate zones. For the second, it is envisioned that a tracer gas system will be needed to confirm that the long-term performance of a WRV system is capable of maintaining a minimum target ventilation rate.

Appendix A
Pressure-Flow Response Plots for Sharp-Edged Orifice Plates

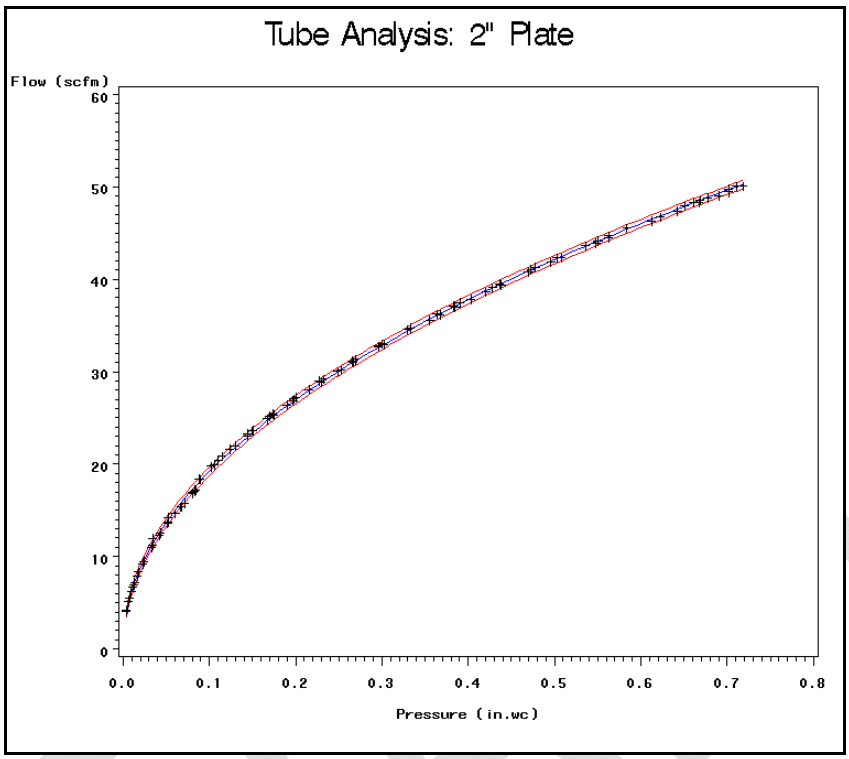

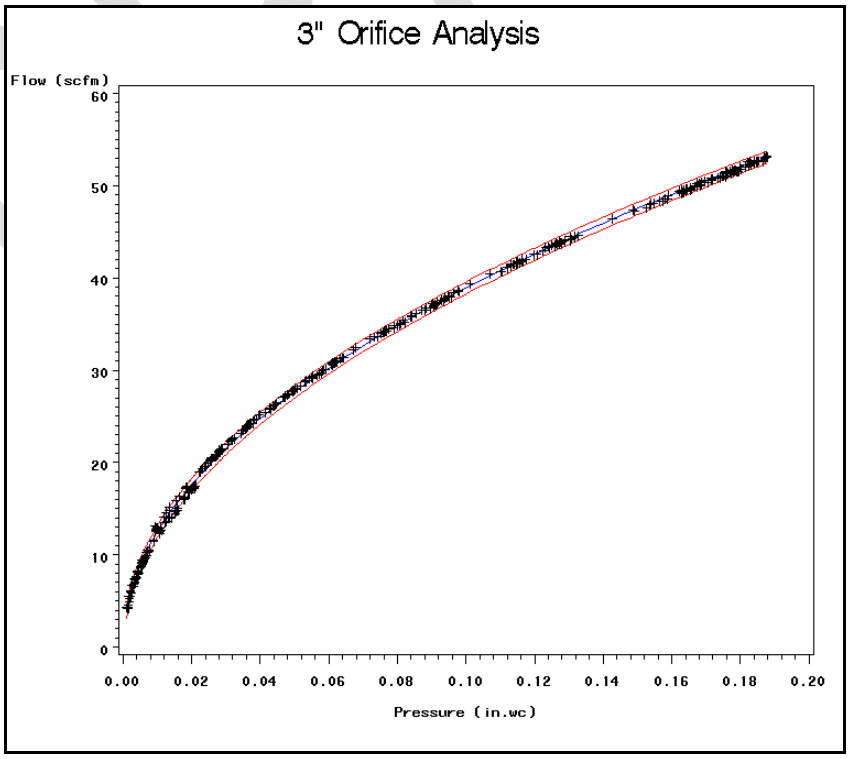

Appendix B
30-Year Annual Weather Factor Results for 8 DOE Climate Zones

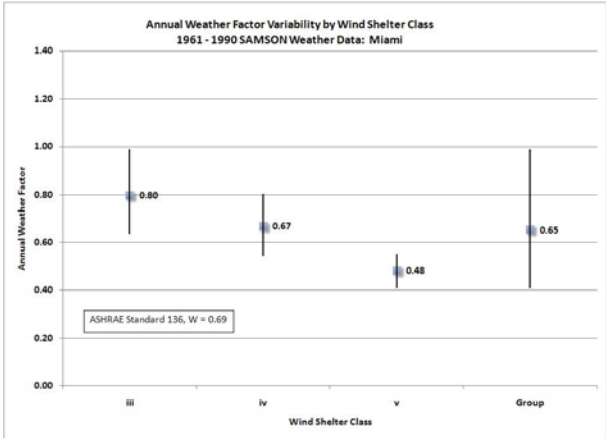

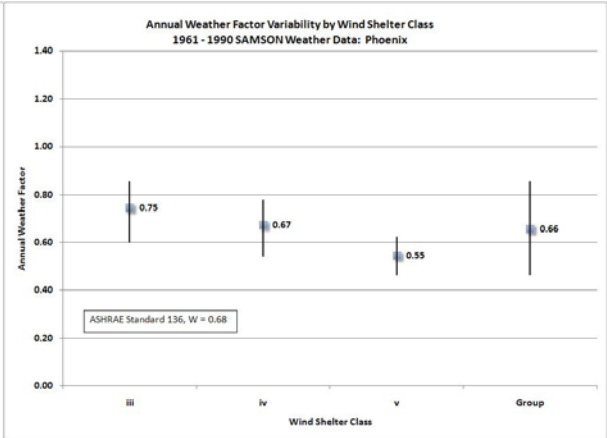

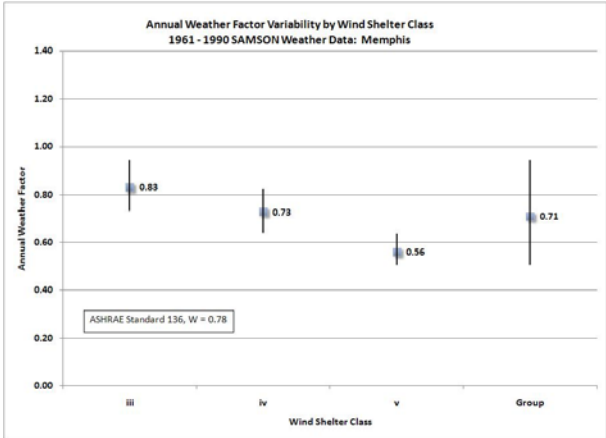

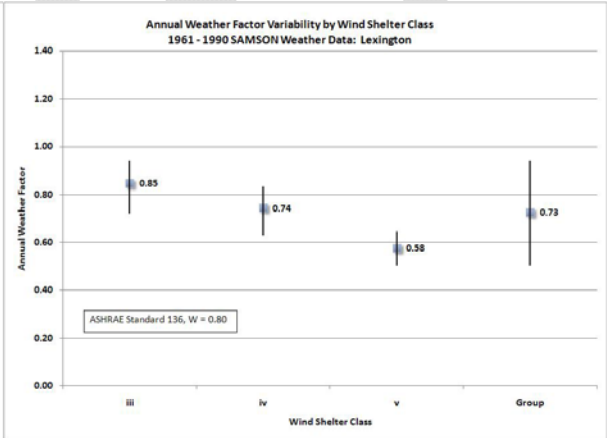

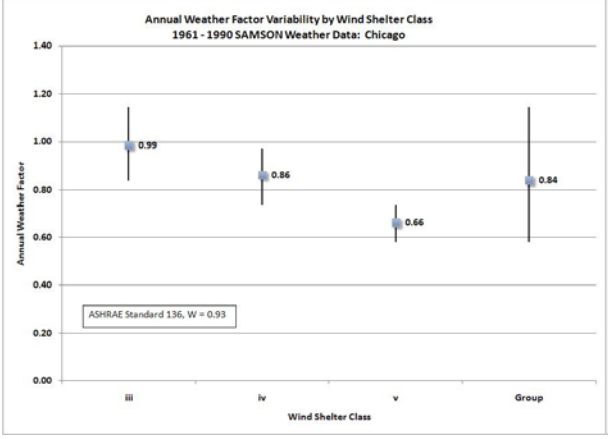

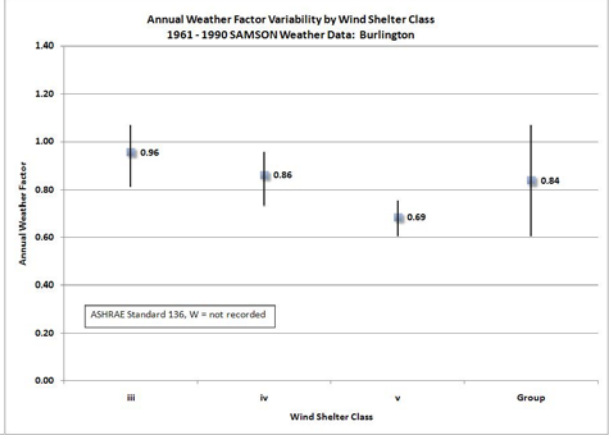

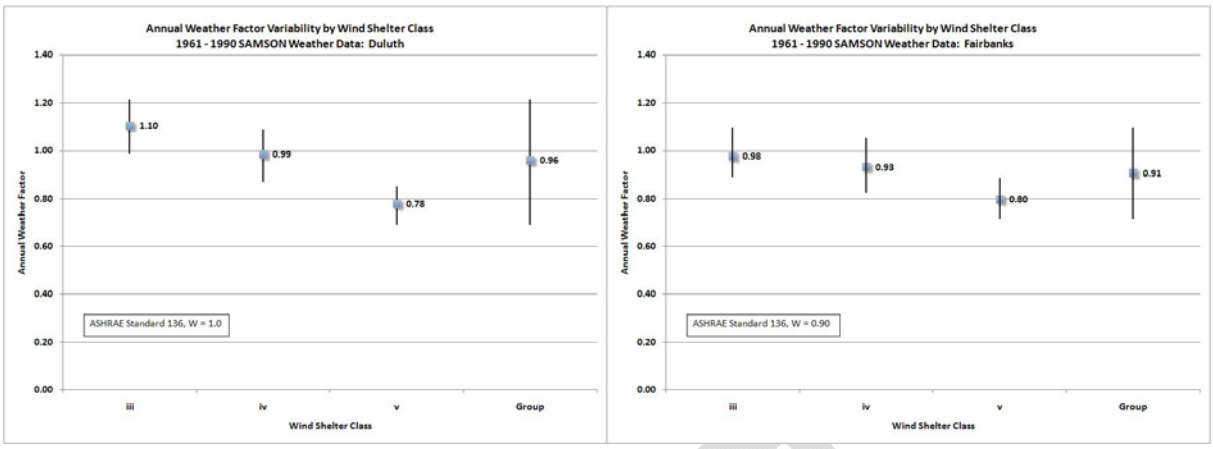
Annual Weather Factor Variability by Wind Shelter Class
1961 - 1990 SAMSON Weather Data: Duluth
Annual Weather Factor
1.40
1.20
1.00
0.80
0.60
0.40
0.20
0.00
1.10
0.99
0.78
0.96
ASHRAE Standard 136, W = 1.0
iii
iv
v
Group
Wind Shelter Class
Annual Weather Factor Variability by Wind Shelter Class
1961 - 1990 SAMSON Weather Data: Fairbanks
Annual Weather Factor
1.40
1.20
1.00
0.80
0.60
0.40
0.20
0.00
0.98
0.93
0.80
0.91
ASHRAE Standard 136, W = 0.90
iii
iv
v
Group
Wind Shelter Class